Superconductor Science and Technology

PAPER

Process to densify $Bi_2Sr_2CaCu_2O_X$ round wire with overpressure before coil winding and final overpressure heat treatment

To cite this article: M R Matras *et al* 2020 *Supercond. Sci. Technol.* **33** 025010

IOP Publishing Superconductor Science and Technology
Supercond. Sci. Technol. 33 (2020) 025010 (9pp) https://doi.org/10.1088/1361-6668/ab5ad6

Process to densify $Bi_2Sr_2CaCu_2O_X$ round wire with overpressure before coil winding and final overpressure heat treatment

M R Matras[1], J Jiang, U P Trociewitz, D C Larbalestier and E E Hellstrom

Applied Superconductivity Center, National High Magnetic Field Laboratory, Florida State University, Tallahassee, FL-32310, United States of America

E-mail: maxime.matras@gmail.com

Received 25 September 2019, revised 5 November 2019
Accepted for publication 22 November 2019
Published 7 January 2020

Abstract

Overpressure (OP) processing of wind-and-react $Bi_2Sr_2CaCu_2O_x$ (2212) round wire compresses the wire to almost full density, decreasing its diameter by about 4% without change in wire length and substantially raising its J_C. However, such shrinkage can degrade coil winding pack density and magnetic field homogeneity. To address this issue, we here present an overpressure predensification (OP-PD) heat treatment process performed before melting the 2212, which greatly reduces wire diameter shrinkage during the full OP heat treatment (OP-HT). We found that about 80% of the total wire diameter shrinkage occurs during the 50 atm OP-PD before melting. We successfully wound such pre-densified 1.2 mm diameter wires onto coil mandrels as small as 10 mm diameter for Ag–Mg-sheathed wire and 5 mm for Ag-sheathed wire, even though such small diameters impose plastic strains up to 12% on the conductor. A further ~20% shrinkage occurred during a standard OP-HT. No 2212 leakage was observed for coil diameters as small as 20 mm for Ag–Mg-sheathed wire and 10 mm for Ag-sheathed wire, and no J_C degradation was observed on straight samples and 30 mm diameter coils.

Keywords: $Bi_2Sr_2CaCu_2O_X$ (2212) round wires, partial-melt process, high temperature superconductor, overpressure, wire densification, solenoid magnets

(Some figures may appear in colour only in the online journal)

1. Introduction

Overpressure (OP) processing $Bi_2Sr_2CaCu_2O_x$ (2212) round wires at 50 atm significantly increased the available critical current density (J_C) to more than 4000 A mm^{-2} at 5 T and 4.2 K [1] and more recently new powders sources have allowed up to 9000 A mm^{-2}, making 2212 performance fully comparable or even superior to the other high temperature superconductors [2]. The increase in J_C is achieved by using an external pressure of 10–100 atm to almost fully densify the 2212 filaments and greatly enhance the superconducting connectivity. As-drawn wires have filaments that are only partially dense because the wire fabrication process requires the 2212 powder particles to slide over one another, limiting their terminal relative density to about 2/3. Melting the wire under 1 atm allows the residual gas in the filament voids to agglomerate into high pressure bubbles which expand and cause the Ag to creep, significantly de-densifying the 2212 [3]. The solution is to perform the melt under 50–100 atm, a pressure which almost completely densifies the filaments, causing the wire diameter to shrink by about 4%. After the full OP heat treatment (OP-HT) (see figure 1(b)), the wire cannot be bent because the 2212 filaments are rigid and brittle. Therefore, the normal wind and react coil-manufacturing process is to wind as-drawn wire into a coil and then apply the OP-HT. A consequence of the 4% wire diameter decrease is that an initially tightly wound coil may become loose. If the wire position shifts, the consequences for

[1] Currently at CERN.

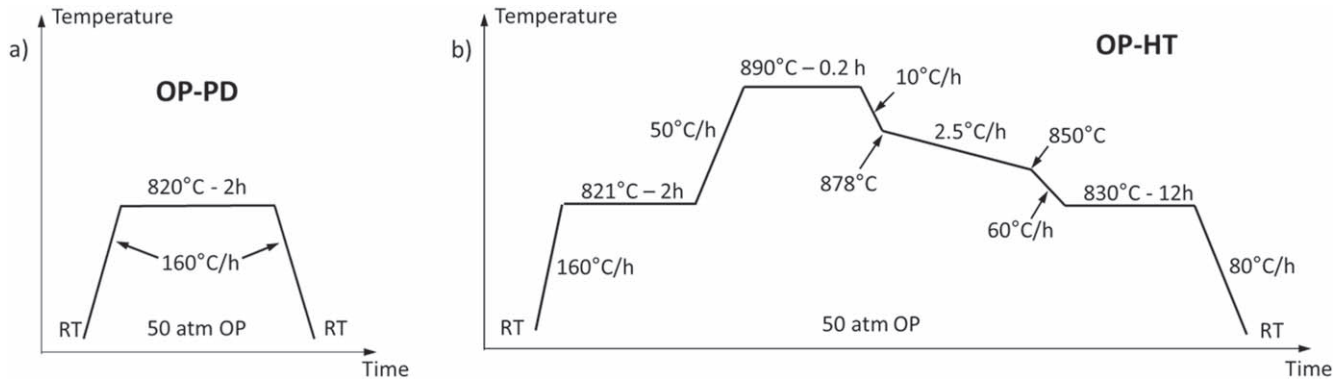

Figure 1. Schematic of the heat treatment schedules for (a) overpressure predensification (OP-PD), and (b) the full overpressure heat treatment (OP-HT). Both heat treatments were done at 50 atm total pressure with PO_2 equal to 0.2, 1.0 and 5.0 atm for OP-PD and 1 atm for OP-HT.

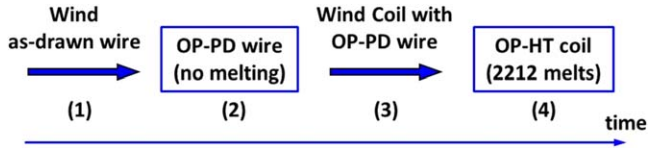

Figure 2. Schematic of the process schedule to form 2212 coils with OP-PD wires. (1) The as-drawn wire is loosely wound on a Al_2O_3 ceramic mandrel and (2) is OP-PDed for 2 h at 50 atm and at 820 °C, below the melting temperature of 2212 powder. (3) The OP-PD wire is unwound and may be insulated. (3) The OP-PD wire is wound into the final coil form and (4) receives an OP-HT at 50 atm with $PO_2 = 1$ atm. The OP-PD was done at 50 atm total pressure with $PO_2 = 0.2$, 1.0, or 5.0 atm.

magnets are significant: the wire may become unsupported and thus damaged, the center of the magnetic field may move, and the field homogeneity may decrease.

As part of a study determining how dense the wires were in the as-drawn condition and what 2212 area was appropriate for normalizing the measured critical current I_c, Matras *et al* [4] showed that the 2212 wire diameter decreased by about 3.3% on heating to 820 °C for 2 h under 50 atm OP (see figure 1(a)). This is roughly 80% of the shrinkage that normally occurs on melting the 2212 during a regular 50 atm OP-HT. At 820 °C, the 2212 filaments remain as unconnected powders with well-defined filament shapes and they can be bent without mechanical damage that would later compromise their electrical properties. Below we refer to the process of densifying the powder before melting as overpressure predensification (OP-PD), while OP-HT describes the overpressure heat treatment process in which the 2212 powder is melted and the superconducting connectivity maximized. In this paper, we investigate the four step process (see figure 2) of (1) pre-winding as-drawn wire, (2) using OP-PD to decrease the wire diameter and densify the 2212 powder below the melting point of 2212, (3) winding a coil with OP-PD wire that is still plastic, and (4) doing the full OP-HT on these coils, while simultaneously paying attention to how these process steps affect J_C. The remarkable finding of our work is that we can wind our 1.2 mm diameter wires around coil forms with diameters as small as 10 mm without any wire leakage, even though the plastic winding strain is then 11%. We found that at least the 30 mm diameter coil showed no loss of J_c performance.

Ag–Mg alloy that can be oxide dispersion strengthened (ODS) is commonly used as the sheath for 2212 wires, as it increases Vicker hardness of Ag–Mg up to a factor 4 compared to pure Ag [5]. To get to the ODS state, the Mg is oxidized to MgO nanoparticles on heating in an oxygen-containing atmosphere. Recognizing that MgO may have a significant impact on the ability to wind OP-PD wire into coils, we compared wires with Ag–Mg and pure Ag sheaths predensified with varying oxygen partial pressure, PO_2, during the OP-PD step and assessed their windability into small diameter coils. Since the PO_2 during OP-PD may significantly affect the ODS properties of the Ag–Mg sheath, we studied $PO_2 = 1.0$ atm as the standard benchmark and used $PO_2 = 0.2$ and 5.0 atm, which are 5 times lower and higher as tests of the role of oxygen partial pressure during the solid-state portion of the total heat treatment.

2. Experimental details

The powder-in-tube 2212 wires were made by Oxford Superconducting Technology (OST) [6, 7] with Nexans granulate powder ($Bi_{2.17}Sr_{1.94}Ca_{0.89}Cu_{2.00}O_{8+x}$). The outer sheath of one wire was Ag-0.2 wt% Mg alloy and the other pure Ag. Both wires had the same double-stack architecture with 18 bundles of 85 filaments with a nominal as-drawn diameter of 1.2 mm. The wires used in this study were about 2.5 m long with both ends hermetically sealed by wrapping a short piece of pure Ag wire around each wire end and then melting it to create the Ag seal.

The process schedule is shown in figure 2. The Ag-sheathed and Ag–Mg sheathed wires (hereafter Ag wire and Ag–Mg wire), were initially co-wound onto a 30 mm diameter Al_2O_3 ceramic mandrel and predensified (figure 1(a)) with varying Ar/O_2 50 atm mixtures ($PO_2 = 0.2$, 1.0, and 5.0 atm). To simulate handling after predensification, we ran the OP-PD wires through our TiO_2 insulation machine [8] with its six 15 cm diameter pulleys (without insulation application though). 50 cm wire sections were cut, their ends

Figure 3. Picture of coils made from OP-PD wire after OP-HT. From left to right, 5, 30, 20, and 10 mm inside diameter coils. The total conductor length is 50 cm for each coil. Each coil has a 6 cm long straight section for I_C measurements. I_C measurements were also done on curved sections of the 30 mm diameter coil.

sealed and then they were wound into four coils with inner diameters of 5, 10, 20 and 30 mm (figure 3). Each coil ended with a 6 cm long straight section used for I_C measurements. The coils were OP-HTed (figure 1(b)) at 50 atm with $PO_2 = 1$ atm. Half-turn sections were also cut from the largest, 30 mm diameter coils for I_C measurements.

The wire diameters of as-received and predensified wires were measured with a laser micrometer (Beta LaserMike AccuScan 5012), which uses the projection of a laser beam to measure the wire diameter along two orthogonal directions perpendicular to the wire. After OP-HTing the coils, the wire diameters of the straight sections were measured with an iNexiv Nikon VMA 2520 light microscope every 0.25 mm along a 2 cm section in the center of the straight section.

For scanning electron microscope (SEM—Zeiss 1540 XB) cross-section imaging, samples were put into conductive epoxy resin and manually dry-polished with SiC papers with decreasing grit size, and then finished for about 12 h using a Buehler Vibromet 2 vibratory polisher with 0.05 μm Al_2O_3 powder mixed with ethanol. The Ag and Ag–Mg wires were etched by dipping the puck into a 2.5:1:2.5 (volume) mixture of NH_4OH (28% – 30%), H_2O_2 (30%), and ethanol for 30 s.

I_C was measured on 4.5 cm long samples from the straight portion of the coils using the four probe technique with a 1 μV cm^{-1} criterion at 4.2 K and 5 T. I_C was also measured on half turns of the 30 mm diameter coils. Half turns from the smaller coils were too small to be measured. Voltage taps were set 1.75 cm from each end and were 1 cm apart. The 2212 area used to calculate J_c followed our normal practice and was the filament area measured on the predensified OP-PD wires where the filaments are still individual and the contrast with the Ag matrix is still good (see figure 6).

3. Results

Figure 4 shows the decrease in wire diameter of all wires as a function of the process conditions. After OP-PD, the as-drawn Ag–Mg wire (figure 4(a)) shows a decrease in wire diameter with increasing PO_2, from 2.6% ± 0.3% at $PO_2 = 0.2$ atm to 3.5% ± 0.6% at $PO_2 = 5.0$ atm, which correspond to 65% and 95% of the total decrease in wire diameter for the standard OP-HT. After OP-HT, the wires heat-treated in all process conditions show similar average decrease in diameter of around 3.7% ± 1.1%. The Ag–Mg reference wire without predensification shrank as much after OP-HT as the wires that underwent OP-PD + OP-HT, with a decrease in diameter of 3.8% ± 0.6%.

After OP-PD in all process conditions, the as-drawn Ag wire (figure 4(b)) shows similar decrease in wire diameter with an average of 3.60% ± 0.62%, which corresponds to an average of 78.9% ± 2.0% of the total decrease in wire diameter. After OP-HT, the reference wire (without OP-PD) shows a decrease in wire diameter of 3.74% ± 0.21%, whereas all wires OP-PDed with $PO_2 = 0.2$, 1.0 and 5.0 atm and then OP-HTed show similar total decrease in wire diameter with an average of 4.37% ± 0.8%. The Ag reference wire without OP-PD decreased less in diameter after OP-HT than the corresponding wire with OP-PD + OP-HT.

The decrease in diameter of Ag–Mg wires in all process conditions after final densification (OP-HT) shows significant standard deviations, suggesting a not fully isotropic densification. In contrast, the Ag wire shows very small decrease in wire diameter standard deviation, suggesting a very isotropic wire densification.

Figure 5 shows the shrinkage of 2.5 m long samples of Ag–Mg and Ag wire OP-PDed with $PO_2 = 1$ atm. The two orthogonal diameter measurements are more similar for the Ag than the alloyed wire (figure 5(b)), whose variations in wire diameter are a little larger, as also observed in figure 4(a). Both should still be considered round. After the full process of OP-PD + OP-HT, both types of wire show similar variations in diameter to those seen after OP-PD.

Cross-sections of the as drawn and OP-PD Ag and Ag–Mg wires in figure 6 that were predensified with $PO_2 = 0.2$ and 1.0 atm showed similar filament microstructures to the as-drawn wire, but the OP-PD wires are denser and smaller in filament cross-sections. The 2212 is still in powder form after OP-PD and has a small amount of secondary phases that was also present in the as-drawn wire. The powder densification during OP-PD gives more contrast between the 2212 powder and the second phases because of the reduced porosity in the filaments. Both types of wire OP-PDed with $PO_2 = 5$ atm show a larger amount of secondary phases (dark regions in figures 6(d) and (h)) compared to the as-drawn wire, suggesting that the 2212 powder partially decomposed on heating. This is consistent with observations made by Scheuerlein *et al* [9] who showed that 2212 powder decomposes above 550 °C for $PO_2 = 5.5$ atm but remains stable for $PO_2 \leqslant 1.0$ atm. EDS analysis showed that secondary phases observed in the wire cross-sections were alkaline earth cuprates and copper-free phases.

Figure 7 shows the sheath grain structure before and after OP-PD at all PO_2 values. The 1–2 μm grain size in the as-drawn Ag–Mg sheath (figure 7(a)) is very uniform but after OP-PD with 0.2 and 5.0 atm O_2, the sheath has an external layer with small grains and an inner layer with large grains that extends towards the pure Ag-matrix surrounding the filaments. With $PO_2 = 0.2$ atm, the external layer is about 7 μm thick and the grains are a few micrometers in size but the inner grains are much larger, varying between about 30 and 110 μm. In contrast, with $PO_2 = 5.0$ atm, the external layer is about 18 μm thick, more than twice as thick but with similar grain size compared to after 0.2 atm OP-PD. The Ag

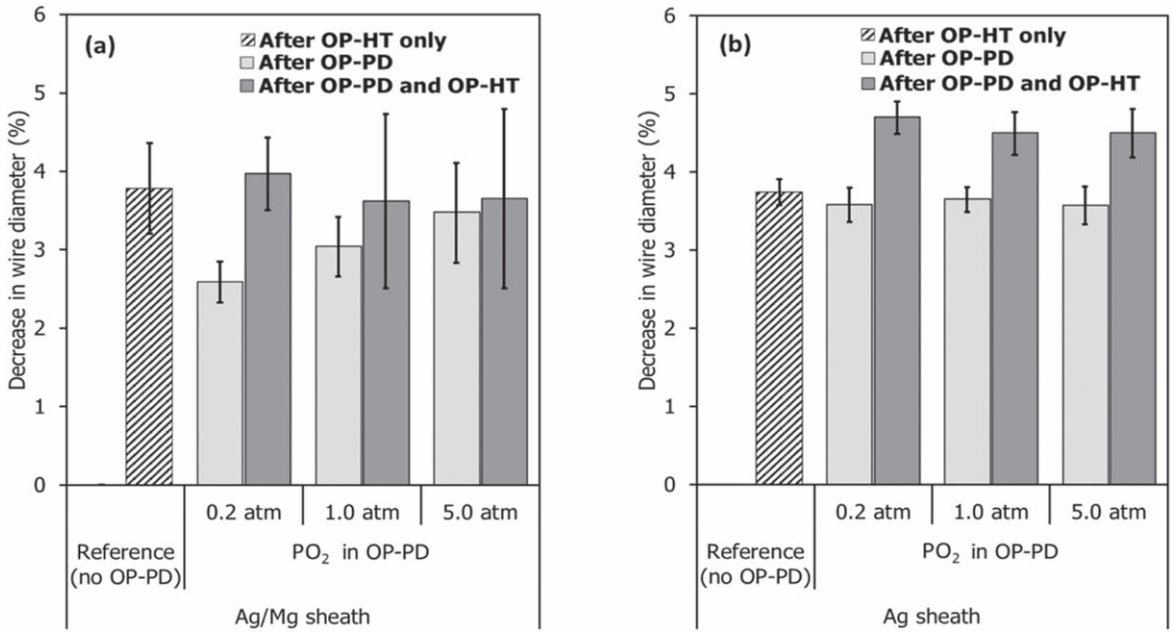

Figure 4. Decrease in diameter of (a) Ag–Mg wires and (b) Ag wires after OP-PD and after OP-PD + OP-HT, compared to the as-received wire (no heat treatment). The OP-PD was done at 50 atm total pressure with $PO_2 = 0.2$, 1.0, and 5.0 atm, and the OP-HT was done at 50 atm with $PO_2 = 1.0$ atm. The reference (no OP-PD) is the decrease in diameter of the OP-HT wire that did not receive OP-PD.

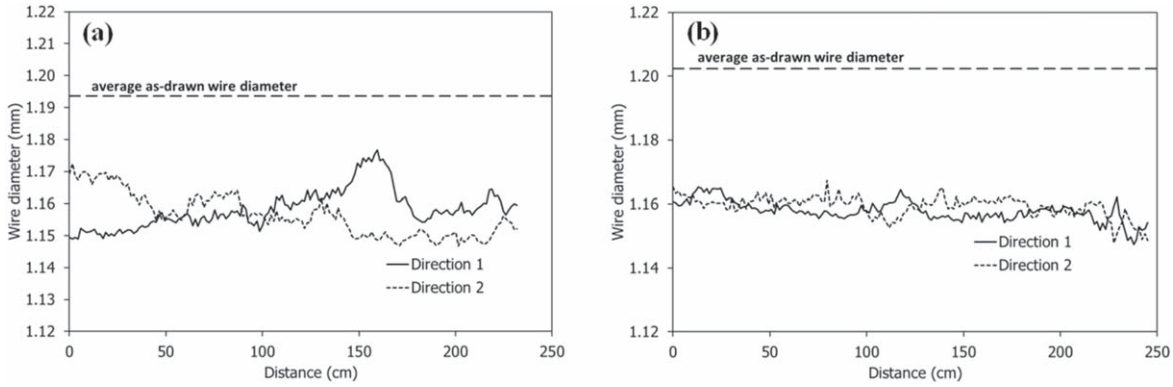

Figure 5. Wire diameter after OP-PD ($PO_2 = 1$ atm) measured in two orthogonal directions across the cross-section along the 250 cm long (a) Ag–Mg wire and (b) Ag wire. The as-drawn wire diameter is shown for reference.

grain size of the internal layer of the 5 atm wire is quite uniform with a size of about 35 μm.

In contrast to the Ag–Mg wires, the Ag wire (figures 7(d)–(f)) shows only one sheath layer of similarly large Ag grains for all samples. The grain size in the as-drawn wire is between about 15 and 45 μm. The grain sizes in the wires OP-PD with $PO_2 = 0.2$ and 5.0 atm are similar and range from about 30 to 145 μm.

Prior to heat treatment, we noticed that the as-drawn Ag–Mg wire was more rigid than the as-drawn Ag wire. Nevertheless, both wires could be wound onto mandrels as small as 5 mm in diameter with very little spring back. After OP-PD, we judged the Ag–Mg wire to be significantly less ductile than the Ag wire, which kept its initial ductility. The stronger OP-PD Ag–Mg wire was more difficult to bend into all the coil diameters and showed significant spring back after winding.

The OP-PD wires were wound into coils and OP-HTed, after which we asked the following two questions: 'Can the OP-PD wire be wound into a coil?' and 'Was the coil leak-free during OP-HT?'

Table 1 summarizes the answers to these two questions. With respect to the first question, the OP-PD Ag wires were successfully wound into all four diameter coils (5, 10, 20 and 30 mm inner dia.) without any sign of cracking, independent of the PO_2 used during OP-PD. The answer for the Ag–Mg wire depended on the PO_2 and the coil diameter. The as-drawn reference wire and the wire predensified (and oxidized) with $PO_2 = 5.0$ atm were successfully wound into all four varying diameter coils. However, the lower PO_2 wires (0.2 and 1.0 atm) cracked when wound into 5 and 10 mm diameter coils. SEM showed cracks only on the tensile side of these wires. Some of the cracks were large (figure 8(a)) and penetrated to the 2212 filaments, which would leak during the OP-HT. Some were small

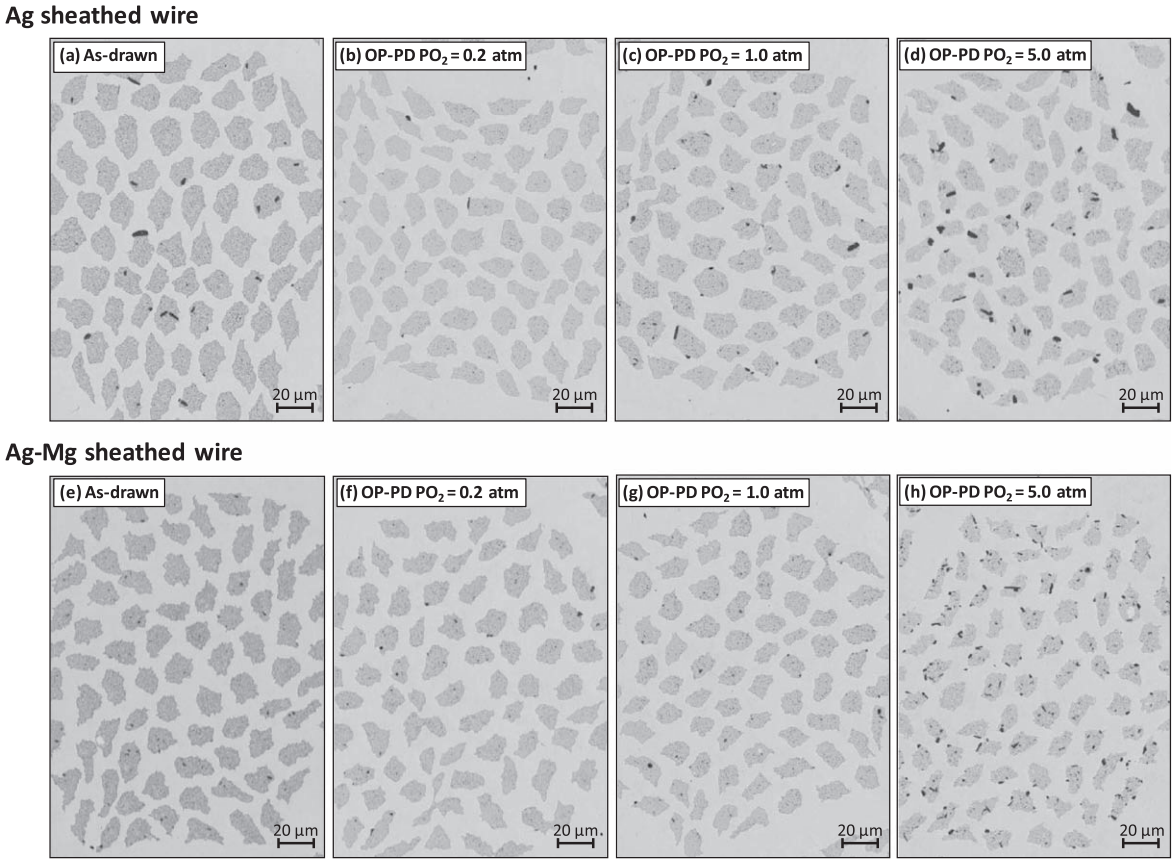

Figure 6. SEM cross-section micrographs of Ag and Ag–Mg wires: (a) and (e) as-drawn wire; wire that was OP-PDed at PO_2 = (b) and (f) 0.2, (c) and (g) 1.0, and (d) and (h) 5.0 atm.

(figure 8(b)) and did not penetrate through the whole sheath thickness and would probably not leak during OP-HT.

The answer to the second question (leak-free OP-HT coil) for Ag wire, is that all coils were leak-free except the 5 mm diameter coil made from wire OP-PDed with $PO_2 = 5.0$ atm, which showed one 2212 leak in the middle of the coil.

For Ag–Mg wire, the 5 and 10 mm diameter coils leaked using wires OP-PDed with $PO_2 = 5.0$ and 1.0 atm, respectively. The rest of the coils were leak-free after OP-HT.

For both the Ag–Mg and Ag wires, the 30 mm diameter coils made with wire OP-PDed with $PO_2 = 0.2$ atm showed 2212 leakage that might have been from forming the coil, or more probably was from touching an adjacent coil made from OP-PD wire that leaked during OP-HT.

Table 2 summarizes the J_C (4.2 K, 5 T) and variation in J_C (ΔJ_C) compared to the reference wire without OP-PD of the straight and curved (30 mm diameter) sections of the coils for all Ag–Mg and Ag wires. Both Ag–Mg and Ag wires, whether straight or curved, show similar qualitative variation in J_C as a function of PO_2 used during OP-PD. J_C increased with increasing PO_2 used during OP-PD. The J_C for the reference Ag–Mg and Ag wires are similar at 4262.9 ± 5.7 A mm^{-2} and 4266.5 ± 13.0 A mm^{-2}, respectively. The Ag–Mg wires OP-PDed with $PO_2 = 1.0$ atm show similar J_C to the reference wires with $\Delta J_C = 2.1\%$ and -1.3% for the straight and curved sections of the coils respectively, showing that OP-PDing Ag–Mg wire with $PO_2 = 1.0$ atm does not affect J_C. After OP-PD with $PO_2 = 0.2$ atm, J_C decreased by 32% and 38%, for the straight and curved sections respectively compared to the reference wires. The Ag–Mg wires OP-PDed with $PO_2 = 5.0$ atm shows an increase in J_C of 22.0% and 22.8% for the straight and curved sections respectively compared to the reference wires. Curved sections of the coils showed very similar J_C values to the straight sections. The n-values in table 2 follow the same trend as J_C as a function of PO_2 with the lowest and highest n-value measured for $PO_2 = 0.2$ atm and 5.0 atm, respectively, for straight section wire with both alloys. In curved sections, the effect of PO_2 on n-value is less significant for Ag–Mg-sheathed samples and not observed for Ag-sheathed samples.

By contrast, the Ag wire was not affected by PO_2 during OP-PD as much as the Ag–Mg wire. A decrease in J_C of 6.7% and 8.3% compared to the reference wire was observed for Ag wires that were OP-PD with $PO_2 = 0.2$ atm. With $PO_2 = 1.0$ and 5.0 atm, Ag wires show similar change in J_C with an increase of 9.3% and 3.7% compared to the reference sample. There is no evidence that $PO_2 = 5.0$ atm during OP-PD provides higher J_C than $PO_2 = 1.0$ atm for Ag wires.

4. Discussion

The OP-PD process described in figure 2 successfully densifies 2212 wire before coil winding and significantly reduces the shrinkage of the wire diameter that occurs during the

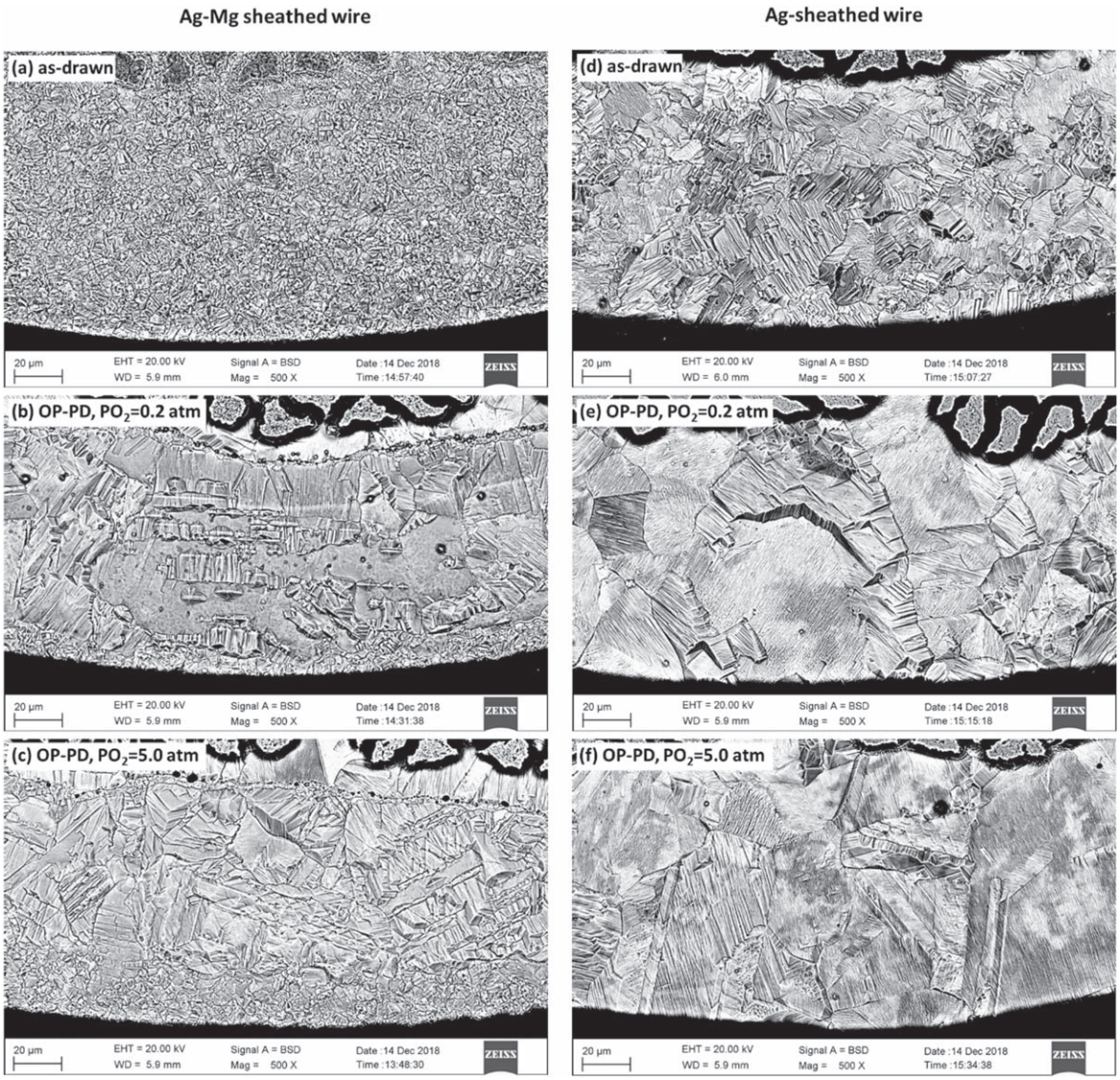

Figure 7. (a)–(c) SEM cross-section micrographs of the Ag–Mg sheath (a) as drawn, and OP-PDed with (b) $PO_2 = 0.2$ atm, and (c) $PO_2 = 5.0$ atm. (d)–(f) Micrographs of the Ag—sheath (d) as-drawn, and, OP-PD with (e) $PO_2 = 0.2$ atm, and (f) $PO_2 = 5$ atm.

subsequent OP-HT of the coil. On average, about 80% of the total diameter decrease occurs during the OP-PD (see figure 1(a)) of Ag–Mg and Ag wires at 50 atm OP with 1 atm PO_2. The remaining 20% decrease in wire diameter occurs during the OP-HT (see figure 1(b)) at 50 atm OP with 1 atm PO_2, as shown in figure 4. Both the Ag and Ag–Mg wire OP-PDed at 50 atm with 1 atm PO_2 can be wound into coils with a diameter as small as 20 mm without cracking during winding and not having leaks after OP-HT. All straight sections and curved sections from 30 mm diameter coils show no decrease in J_C, as shown in table 2. Our process is therefore suitable for 2212 magnet OP-processing and can be used for coils, made from Ag and Ag–Mg wires, with an inner diameter larger than 20 mm.

During OP-PD at $PO_2 = 0.2$, 1.0, and 5.0 atm (see figures 4 and 5 and in [2]), both Ag–Mg and Ag wires show significant decrease in wire diameter below the melting temperature of the 2212 precursor powder. The fact that Ag wire showed a very homogeneous decrease in diameter, whereas the Ag–Mg wire showed slight variations in the decrease in wire diameter along its length, indicates a non-uniformly densified wire. This may indicate an inhomogeneous sheath hardness in the Ag–Mg wire caused by an inhomogeneous distribution of the MgO particles that occurs as the MgO grains form during the heat treatments, as shown in [10]. The oxidation of Mg during the OP-PD may be homogeneous, but as the MgO particles grow during the OP-PD they may become inhomogeneously distributed in the sheath, especially at Ag grain boundaries [11], leading to variations in hardness from place to place within the Ag–Mg sheath. This variation in hardness may cause non-uniform deformation of the wire under the applied hydrostatic pressure.

As-drawn and OP-PD Ag wires, as well as as-drawn Ag–Mg wire can be wound into coils with a diameter as small as 5 mm independent of PO_2 used during OP-PD despite the large plastic bending deformation. In contrast, the Ag–Mg wire OP-PDed with 0.2 and 1.0 atm PO_2 cracked when

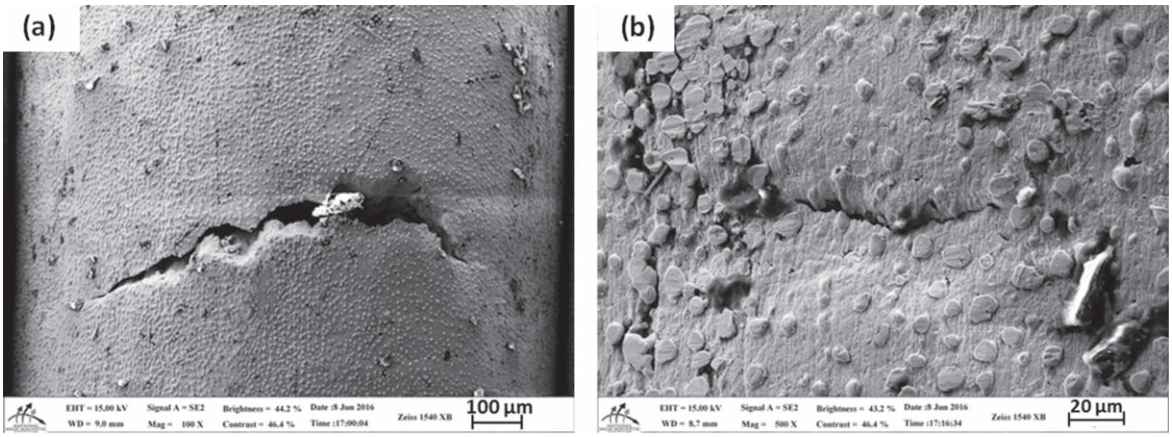

Figure 8. SEM secondary electron micrographs of the surface on the tension side of a Ag–Mg wire wound into a 5 mm diameter coil after OP-PD (PO_2 = 0.2 atm). (a) Macro and (b) micro cracks are visible on the surface of the Ag–Mg sheath.

Table 1. Summary of the answers to the two questions: Can the OP-PD wire be wound into 5, 10, 20 and 30 mm diameter coils? Is the coil wound with OP-PD wire leak-free during OP-HT? The answers are tabulated for Ag–Mg and Ag-sheathed wires, and for reference wires that received no OP-PD. We did not OP-HT the two coils that were obviously damaged during winding (Ag–Mg wire, OP-PDed at PO_2 = 0.2 and 1.0 atm, 5 mm diameter coil). Y or N = answer is yes or no. A question mark indicates that the source of the 2212 leak is not clearly identified, as discussed in the text.

Wire sheath	PO_2 for OP-PD	Can the OP-PD wire be wound into a coil?				Is the coil leak-free after OP-HT?			
		Coil diameter (mm)				Coil diameter (mm)			
		5	10	20	30	5	10	20	30
Ag–Mg	Reference (no OP-PD)	Y	Y	Y	Y	Y	Y	Y	Y
	0.2 atm	No	Y	Y	Y	*	Y	Y	?
	1.0 atm	No	Y	Y	Y	*	No	Y	Y
	5.0 atm	Y	Y	Y	Y	No	Y	Y	Y
Ag	Reference (no OP-PD)	Y	Y	Y	Y	Y	Y	Y	Y
	0.2 atm	Y	Y	Y	Y	Y	Y	Y	?
	1.0 atm	Y	Y	Y	Y	Y	Y	Y	Y
	5.0 atm	Y	Y	Y	Y	No	Y	Y	Y

*Coils were not OP-HTed.

winding the 5 mm diameter coil. This limitation in bending diameter is due to the ODS of the Ag–Mg sheath during OP-PD. The Ag–Mg wire OP-PDed with PO_2 = 5.0 atm was qualitatively as stiff as the Ag–Mg wires OP-PDed with 0.2 and 1.0 atm, but could be wound to 5 mm diameter coil with no evidence of sheath cracking. It suggests non-intuitively that Ag–Mg wire OP-PDed with high oxygen content (PO_2 = 5 atm) retains more of its ductility when ODS occurs during OP-PD than the wires OP-PDed with low oxygen content (0.2 and 1.0 atm O_2). One possible explanation is that the MgO particle growth process competes with Ag grain growth with increasing temperature [12]. If Mg oxidation occurs before the Ag grains grow, the MgO particles pin the Ag grains, limiting their grain growth. In contrast, if Mg oxidation is slow, MgO forms in already large Ag grains. Prorock *et al* [13] showed that the rate of Mg oxidation increases with increasing PO_2, which we assume also occurs in our samples. Therefore with PO_2 = 0.2 atm, Mg oxidizes slower than with PO_2 = 5 atm and Ag grain growth dominates and forms large Ag grains, resulting in fewer, but longer Ag grain boundaries. This is consistent with figure 7 and [14] that show cross-sections of 2212 wire predensified at PO_2 = 0.2 atm with a thin layer of small grains near the outer surface and very large grains with long grain boundaries, oriented radially, deeper in the sheath. Because of slow Mg oxidation, MgO may not have migrated yet and therefore the long grain boundaries are much softer than the large Ag grains with MgO particles and are preferential paths for crack propagation in the hardened sheath [15, 16]. In contrast, in samples OP-PDed with PO_2 = 5 atm, Mg oxidizes more rapidly and deeper into the sheath than with PO_2 = 0.2 atm, preventing the growth of large Ag grains and increasing the Ag grain boundary density within the sheath, as shown in figures 7(b), (c) and [14]. The larger number of Ag grain boundaries in the Ag–Mg wire with PO_2 = 5 atm may limit the crack propagation [15, 16] through the sheath and increase the ductility of the overall sheath relative to the Ag–Mg wire with PO_2 = 0.2 atm. In addition, Prorok *et al* [13] also show that the Knoop hardness decreases with increasing grain size of Ag–Mg alloy, which suggests that large grain Ag–Mg matrix would be more likely to rupture under tensile stress than small grain matrix.

Table 2. Summary of J_C(4.2 K, 5 T), n value and ΔJ_C (change in J_C compared to $J_{C\ ref}$ of the reference samples with no OP-PD) of the straight and curved sections (from 30 mm diameter coils) of the (a) Ag–Mg and (b) Ag wire coils OP-HTed with $PO_2 = 1$ atm.

(a) Ag–Mg sheathed wire		
PO_2 during OP-PD	Straight section	Curved section
	ΔJ_C (%)	
0.2 atm	−31.7	−38.0
1.0 atm	2.1	−1.3
5.0 atm	22.0	22.8
	J_C (Amm^{-2})	
Reference (no OP-PD)	4303.5 ± 14.6	4262.9 ± 5.7
0.2 atm	2939.0 ± 3.7	2667.7 ± 7.3
1.0 atm	4394.9 ± 10.2	4249.1 ± 16.7
5.0 atm	5248.4 ± 12.2	5282.9 ± 9.3
	n-value	
Reference (no OP-PD)	26.5 ± 1.0	24.6 ± 0.5
0.2 atm	21.1 ± 0.3	17.9 ± 0.4
1.0 atm	23.8 ± 0.6	24.1 ± 0.9
5.0 atm	29.8 ± 1.0	23.8 ± 0.7
(b) Ag sheathed wire		
PO_2 during OP-PD	Straight section	Curved section
	ΔJ_C (%)	
0.2 atm	−6.7	−8.3
1.0 atm	3.0	7.9
5.0 atm	9.3	3.7
	J_C (Amm^{-2})	
Reference (no OP-PD)	4219.9 ± 2.8	4266.5 ± 13.0
0.2 atm	3935.1 ± 30.9	3870.1 ± 7.7
1.0 atm	4346.6 ± 27.2	4555.0 ± 3.7
5.0 atm	4614.3 ± 10.6	4376.2 ± 4.5
	n-value	
Reference (no OP-PD)	28.2 ± 0.1	23.1 ± 0.5
0.2 atm	22.7 ± 1.6	23.9 ± 0.4
1.0 atm	24.0 ± 1.3	26.4 ± 0.3
5.0 atm	29.1 ± 0.6	21.8 ± 0.3

Surprisingly, we also found that using $PO_2 = 5$ atm during OP-PD increases J_C by 22% after OP-HT in Ag–Mg wires and about 9% in Ag wires compared to the reference OP-HT wires. Therefore a magnet made with Ag–Mg wire may be first OP-PD heat treated (see figure 1(a)) at 50 atm OP with $PO_2 = 5$ atm before the OP-HT (see figure 1(b)), with or without unwinding the conductor, to increase the J_C of the 2212 wire by about 22%. We caution that we do not understand why an increase in J_C occurs and we strongly expect this result to be wire dependent.

The mechanisms responsible for the J_C variation in both Ag and Ag–Mg wires is not clear but it seems connected to the ODS of the sheath for Ag–Mg wires. Changing PO_2 during OP-PD of Ag wire has little effect on J_C (table 2), whereas J_C of Ag–Mg wire shows a very strong dependence on PO_2 during OP-PD decreasing by 38.0% ($PO_2 = 0.2$ atm) and increasing by 22.8% ($PO_2 = 5$ atm) compared to $PO_2 = 1$ atm during OP-PD. This suggests that the mechanism responsible for this variation in J_C occurs during OP-PD and depends on the PO_2. Further, the fact that the Ag–Mg wires OP-PD at the three PO_2s were all OP-HTed with the same $PO_2 = 1$ atm shows that what occurs during OP-PD cannot be reversed when OP-HTing with $PO_2 = 1$ atm. This effect may be due to the reaction between Cu, which has the highest diffusion coefficient of the cations in 2212 [17, 18], and Mg forming (Mg, Cu)O.

5. Summary

We have studied winding and over-pressure (OP) processing 2212 solenoid coils using predensified wire made by OP-PD (overpressure predensification), which compresses the wire below the melting point of 2212. The OP-PD minimizes the decrease in wire diameter during the final OP-HT (overpressure heat treatment) of the coil. We found that about 80% of the total decrease in wire diameter occurs during the OP-PD at 820 °C for 2 h at 50 atm. The OP-PD wire can be wound into coils with an inner diameter as small as 20 mm for Ag–Mg-sheathed 2212 wire and 10 mm for Ag-sheathed 2212 wire with no 2212 leakage. No J_C degradation was observed after the OP-HT of the straight sections and 30 mm diameter coil at 50 atm OP with $PO_2 = 1$ atm. Using $PO_2 = 5.0$ atm during OP-PD significantly increases J_C by 22%, compared to the reference wire that is OP-HTed without OP-PD (standard OP-HT).

Acknowledgments

This work was supported by a grant from the US Department of Energy, Office of High Energy Physics (DE-SC0010421) and from the NHMFL, which is supported by the NSF under NSF/DMR-1157490 and 1644779 and by the State of Florida. Research reported in this publication was also supported by the National Institute of General Medical Sciences of the National Institutes of Health under Award Number R21GM111302. The content is solely the responsibility of the authors and does not necessarily represent the official views of the National Institutes of Health. A special acknowledgment to US CDP, to T Shen of LBNL for providing the Ag wire and to our collaborators within the BSCCO strand and cable collaboration (BSCCo), to colleagues at Bruker OST, and to C Matis, A Francis, B Chew, J Lu, P Chen, and J Gillman at ASC for technical support. Frequent discussions with other members of the ASC 2212 group are gratefully acknowledged too.

ORCID iDs

M R Matras https://orcid.org/0000-0003-4613-2837
E E Hellstrom https://orcid.org/0000-0001-8263-8662

References

[1] Larbalestier D C *et al* 2014 Isotropic round-wire multifilament cuprate superconductor for generation of magnetic fields above 30 T *Nat. Mater.* **13** 375–81

[2] Jiang J *et al* 2019 High-performance Bi-2212 round wires made with recent powders *IEEE Trans. Appl. Supercond.* **29** 6400405
[3] Shen T, Ghosh A, Cooley L and Jiang J 2013 Role of internal gases and creep of Ag in controlling the critical current density of Ag-sheathed $Bi_2Sr_2CaCu_2O_x$ wires *J. Appl. Phys.* **113** 213901
[4] Matras M R, Jiang J, Larbalestier D C and Hellstrom E E 2016 Understanding the densification process of $Bi_2Sr_2CaCu_2O_x$ round wires with overpressure processing and its effect on critical current density *Supercond. Sci. Technol.* **29** 105005
[5] Maeda H 1996 *Bismuth-Based High-Temperature Superconductors* (New York: CRC Press) 9780824796907
[6] Rikel M O *et al* 2006 Effect of composition on the melting behaviour of Bi2212-Ag conductors *J. Phys. Conf. Ser.* **43** 51
[7] Miao H *et al* 2006 Studies of precursor composition effect on J_C in Bi-2212/Ag wires and tapes *AIP Conf. Proc.* **824** 673–82
[8] Kandel H *et al* 2015 Development of TiO_2 electrical insulation coating on Ag-alloy sheathed $Bi_2Sr_2CaCu_2O_{8-x}$ round-wire *Supercond. Sci. Technol.* **28** 035010
[9] Scheuerlein C *et al* 2016 Influence of the oxygen partial pressure on the phase evolution during Bi-2212 wire melt processing *IEEE Trans. Appl. Supercond.* **26** 6400304
[10] Hossain I *et al* 2017 Effect of sheath material and reaction overpressure on Ag extrusions into the TiO_2 insulation coating of Bi-2212 round wire *IOP Conf. Ser.: Mater. Sci. Eng.* **279** 012021
[11] Goldacker W, Mossang E, Quilitz M and Rikel M 1997 On the phase formation in Ag and AgMg sheathed BSCCO (2223) tapes *IEEE Trans. Appl. Supercond.* **7** 1407–10
[12] Prorok B C, Park J H, Goretta K C, Koritala R E, Balachandran U and McNallan M J 2001 Internally oxidized Ag/1.2 at% Mg sheaths for Bi-2223 tapes *IEEE Trans. Appl. Supercond.* **11** 3273–6
[13] Prorok B C, Goretta K C, Park J-H, Balachandran U and McNallan M J 2002 Oxygen diffusion and internal oxidation of Mg in Ag/1.12at%Mg *Physica* C **370** 31–8
[14] Matras M, Jiang J, Chen P, Kametani F, Trociewitz U P, Hellstrom E E and Larbalestier D C 2015 Densification and pre-densification of 2212 round wires with over-pressure processing *The European Conf. on Applied Superconductivity (Lyon, France, 09-September)*
[15] Lawn B R 1975 *Fracture of Brittle Solids* (*Cambridge Solid State Science Series*) (Cambridge: Cambridge University Press)
[16] Sukumar N and Srolovitz D J 2004 Finite element-based model for crack propagation in polycrystalline materials *Comput. Appl. Math.* **23** 363–80
[17] Shen T 2010 Processing, microstructure, and critical current density of Silver-sheathed $Bi_2Sr_2CaCu_2O_x$ multifilamentary round wire *PhD Thesis* Florida State University
[18] Wesolowski D E, Rikel M O, Jiang J, Arsac S and Hellstrom E E 2005 Reactions between oxides and Ag-sheathed $Bi_2Sr_2CaCu_2O_x$ conductors *Supercond. Sci. Technol.* **18** 934